Surface & Coatings Technology 408 (2021) 126789

Contents lists available at ScienceDirect

Surface & Coatings Technology

journal homepage: www.elsevier.com/locate/surfcoat

Effect of laser re-melting on geometry and mechanical properties of YCF102 cladding layer

Wenchao Xi, Boxue Song, Zixuan Wang, Tianbiao Yu *, Jun Wang, Yuanxing Dai

School of Mechanical Engineering and Automation, Northeastern University, PR China

ARTICLE INFO

Keywords:
Laser re-melting
Morphology
Microstructure
Microhardness
Wear resistance

ABSTRACT

The aim of this paper is to investigate the effect of laser re-melting on the morphology and mechanical properties of cladding layer under different laser power conditions. In this study, the laser re-melting tests were performed on YCF102 cladding layer with different laser power, and the morphology and microstructure of each cladding layer were researched by optical microscopy. Meanwhile, the microhardness and wear resistance of YCF102 cladding layer after laser re-melting with different laser power were studied. The results show that laser re-melting can not only improve the morphology of cladding layer, but also improve the microhardness and wear resistance of cladding layer. However, the excessive re-melting laser power leads to the increase of the number of defects in the cladding layer and the deterioration of the mircrohardness and wear resistance of cladding layer. When the re-melting laser power is 650 W, the cladding layer not only has a small surface roughness and no defects, but also has good mechanical properties.

1. Introduction

Laser cladding is a kind of surface modification technique in which the alloy powder is rapidly melted on the surface of substrate by laser irradiation. With the advantages of small heat-affected zone, well metallurgical combination with substrate and low cost, it has attracted more and more attention [1–3]. Currently, laser cladding has been applied in aerospace, repair of damaged machine tools and automotive industry [4,5]. However, many problems still exist in the application of laser cladding, and forming quality is one of the key factors restricting the development of laser cladding.

In the laser cladding process, there are many defects in forming quality such as incomplete melting powder, pores and cracks. In order to improve the forming quality, some researches aiming at the relationship between process parameters and forming quality of laser cladding [6–8] were conducted. Some scholars also improved the forming quality of laser cladding by adding ceramic phase, changing material form and controlling heat rate [9–11]. Although there are many different methods to improve the forming quality, the effect is not obvious. As a new technology to improve the forming quality of laser cladding, laser re-melting has attracted more and more attention. Yu et al. [12] studied the effect of laser re-melting strategy on the surface roughness and porosity of cladding layer, and the results showed that the optimization of laser re-melting strategy can effectively reduce the surface roughness of cladding layer. Laser re-melting can also eliminate the number of pores in the cladding layer, shorten the process cycle and achieve the purpose of reducing cost of secondary operations [13,14]. In addition, the microstructure and phase composition of re-melted cladding layer were also studied. Sun et al. [15] presented that the microstructure of cladding layer after laser re-melting is more uniform and finer, and has a significant impact on the element distribution in the cladding layer. Gao et al. [16] studied the relationship between re-melting laser scanning speed and microstructure of cladding layer, and the results showed that the increase of re-melting laser scanning speed leads to the decrease of the area and crystalline size of refined zone. Cai et al. [17] confirmed that laser re-melting has no effect on the phase composition of the Ni-Cr-Co-Ti-V high entropy alloy coating, but the wear resistance is improved. In addition, Yao et al. [18] confirmed that laser re-melting has a significant effect on the surface mechanical properties. Moreover, Balla et al. [19] confirmed that laser surface melting can significantly improve the surface hardness and wear resistance. Laser surface melting can also improve the surface hardness of AISI 410 stainless steel [20]. Zhou et al. [21] studied the effect of laser re-melting on the corrosion resistance and microhardness of in-situ WC reinforced Fe-based amorphous composite coating, and the results showed that the re-melted composite coating has good corrosion resistance and higher microhardness. Xin et al. [22]

* Corresponding author.
E-mail address: neutianbiaoyu2018@gmail.com (T. Yu).

https://doi.org/10.1016/j.surfcoat.2020.126789
Received 13 January 2020; Received in revised form 19 December 2020; Accepted 21 December 2020
Available online 2 January 2021
0257-8972/© 2020 Elsevier B.V. All rights reserved.

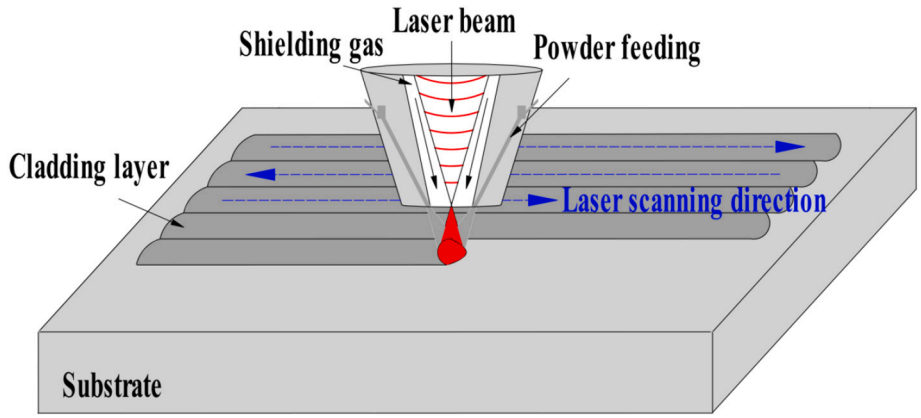

Fig. 1. Schematic diagram of laser cladding and coaxial powder feeding.

Table 1
Chemical composition of the YCF102 alloy powder and AISI1045 steel (wt%) (provided by manufacturer).

Powder model	C	Si	Mn	Ni	Cr	N	Mo	Nb	Cu	P,S	Fe
YCF102	0.05	0.9	0.4	6.5	15.5	0.22	1.0	0.31	–	–	Bal.
AISI1045 steel	0.42–0.5	0.17–0.37	0.5–0.8	≤0.25	≤0.25	–	–	–	≤0.25	≤0.045	Bal.

presented that laser re-melting can enhance the bonding between adjacent layers, thereby improving the tensile strength and yield strength.

The current research mainly focuses on the comparison and analysis of the morphology and properties of re-melted and unremelted cladding layers, while the research on the forming characteristics and mechanical properties of re-melted cladding layers after different laser power re-melting should also be addressed. Therefore, the forming characteristics and mechanical properties of YCF102 coating after re-melting under different laser power conditions were systematically explored and analyzed.

2. Experimental details

The laser cladding system of this research consists of an IPG fiber continuous wave pulsed laser generator (YLR-1000W), a vertical machining center (VMC1100P), a set of water-cooling system and powder feeding system. The laser generator is produced by Anhui Yuchen Laser Technology Co., Ltd., with the spot diameter of 1.1 mm. The laser wavelength used in the experiments ranges from 1070 nm up to 1080 nm. The laser generator is installed on vertical machining center, and the powder feeding mode is coaxial powder feeding as shown in Fig. 1. The injection angle of powder is 31.41°. In order to ensure the performance of cladding layer and the well metallurgical bond between cladding layer and substrate, the distance from the laser nozzle to the substrate is fixed at 16 mm. Due to high processing temperature during laser cladding, alloy powder and substrate undergo oxidation reaction, resulting in a decrease in the properties. To avoid this phenomenon, argon gas is used as shielding gas and powder feeding gas, and the powder is flowed by 6 l/min of the argon gas to form a powder flow.

Considering AISI1045 steel is often used in machine tool parts, the substrate is an AISI1045 steel plate of medium carbon content with the dimensions of 110 mm (Length) × 120 mm (Width) × 10 mm (Thickness). To ensure the surface of substrate is flat and clean, the surface of substrate is ground with metallographic sandpaper. Then, the impurities and oil stains on the surface are removed by acetone and alcohol. YCF102 is an Fe-based alloy powder (100–270 mesh) produced by Anhui Yuchen Laser Technology Co., Ltd. Because of its low cost, high hardness and wear resistance, similar linear expansion coefficient and well metallurgical bond with the substrate, it is widely used in the field of repairing machine tool damaged parts. The composition of YCF102 alloy powder and substrate material is shown as Table 1.

According to the previous experimental results, when the laser power is from 550 W to 850 W, the cladding layer has good morphology. Therefore, 550 W to 850 W were used as the re-melting laser power. The process parameters of laser cladding and re-melting are shown in Table 2. In the process of laser re-melting, argon gas was still used as shielding gas. The spot diameter is 1.1 mm, and the defocusing amount is 16 mm. After the experiments, the cross section of each sample was obtained by wire electrical discharge machining (WEDM), and the top layer of each sample was removed by grinding machine for wear resistance tests. The cross section of each sample was ground by metallographic sandpaper, and then it is polished by a polisher. Finally, the microstructure of each sample was obtained after it was etched by aqua regia.

Surface morphology and microstructure of each sample was researched by optical microscopy (OM). In terms of mechanical properties, the micro-hardness of each sample was measured by MH-500 Micro-hardness tester with a load of 10 N and a loading time of 10s. In addition, the wear resistance of each sample was measured by MFT-4000 multifunctional material surface performance tester, and wear track was measured by Olympus 3D measuring laser microscope (OLS4100). To avoid the large error of weighting method before and after wear test, the wear weight was calculated by the volume function.

Table 2
The process parameters of laser cladding and re-melting.

No.	Laser power (W)	Powder feeding rate (g/min)	Laser scanning velocity (mm/s)	Re-melting laser power (W)	Re-melting laser scanning velocity (mm/s)
1	750	7	4	–	–
2	750	7	4	550	4
3	750	7	4	650	4
4	750	7	4	750	4
5	750	7	4	850	4

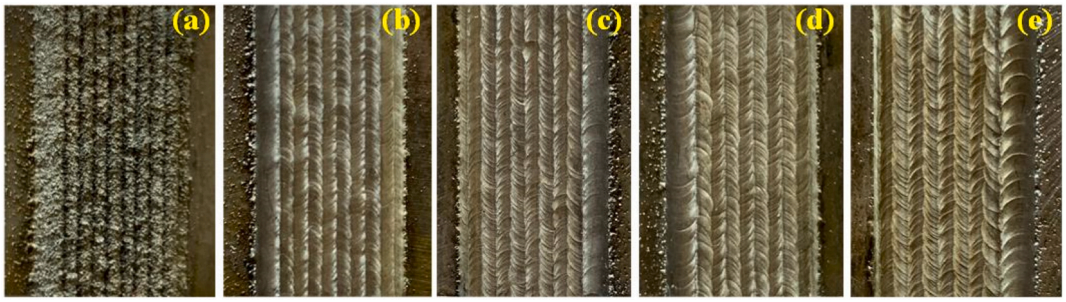

Fig. 2. The surface morphology of cladding layer of (a) Sample No.1; (b) Sample No.2; (c) Sample No.3; (d) Sample No.4; (e) Sample No.5.

3. Results and discussion

3.1. Surface morphology

Fig. 2 shows the surface morphology of different samples. It is noticed that the morphology of each sample is obviously different. As shown in Fig. 2(a), there are many incompletely melted particulate alloy powders on surface of YCF102 cladding layer without laser re-melting, resulting in a rougher surface. Possible reasons of this phenomenon may be concluded as: (1) Due to a part of alloy powder collides in the laser beam, the part of alloy powder is irradiated for a short time in the laser beam, which leads to the part of alloy powder to be not completely melted and adhered to the cladding surface. (2) A part of alloy powder is still fallen on the surface of cladding layer after the laser beam moves away. This phenomenon is caused by short laser irradiation time for this part of alloy powder in the laser beam. In addition, the overlapping marks between each cladding track are obvious. Due to a longer distance between the overlapped region and the focus of laser beam, the alloy powder of this region is subjected to a relatively weak laser irradiation, which results in a less amount of powder melted in this area. Fig. 2(b), (c), (d) and (e) show the surface morphology of cladding layer after different laser power re-melting. It is noticed that the incompletely melted alloy powders on surface of cladding layer disappear. Moreover, the overlapping marks between each cladding track are less obvious, and the surface of cladding layer is smoother. The cause of this phenomenon can be concluded as: when the laser beam passes through the surface again, the cladding layer and the incompletely melted alloy powder are melted and solidified again, resulting in a smoother cladding layer.

Fig. 3 shows the three-dimensional optical profile of the cladding layer with different samples. As shown in Fig. 3(a), the surface of the cladding layer without laser re-melting is very rough. However, the surface of cladding layer after different laser power re-melting is smooth as shown in Fig. 3(b), (c), (d) and (e). As shown in Fig. 4, the surface roughness of cladding layer after different laser power re-melting is

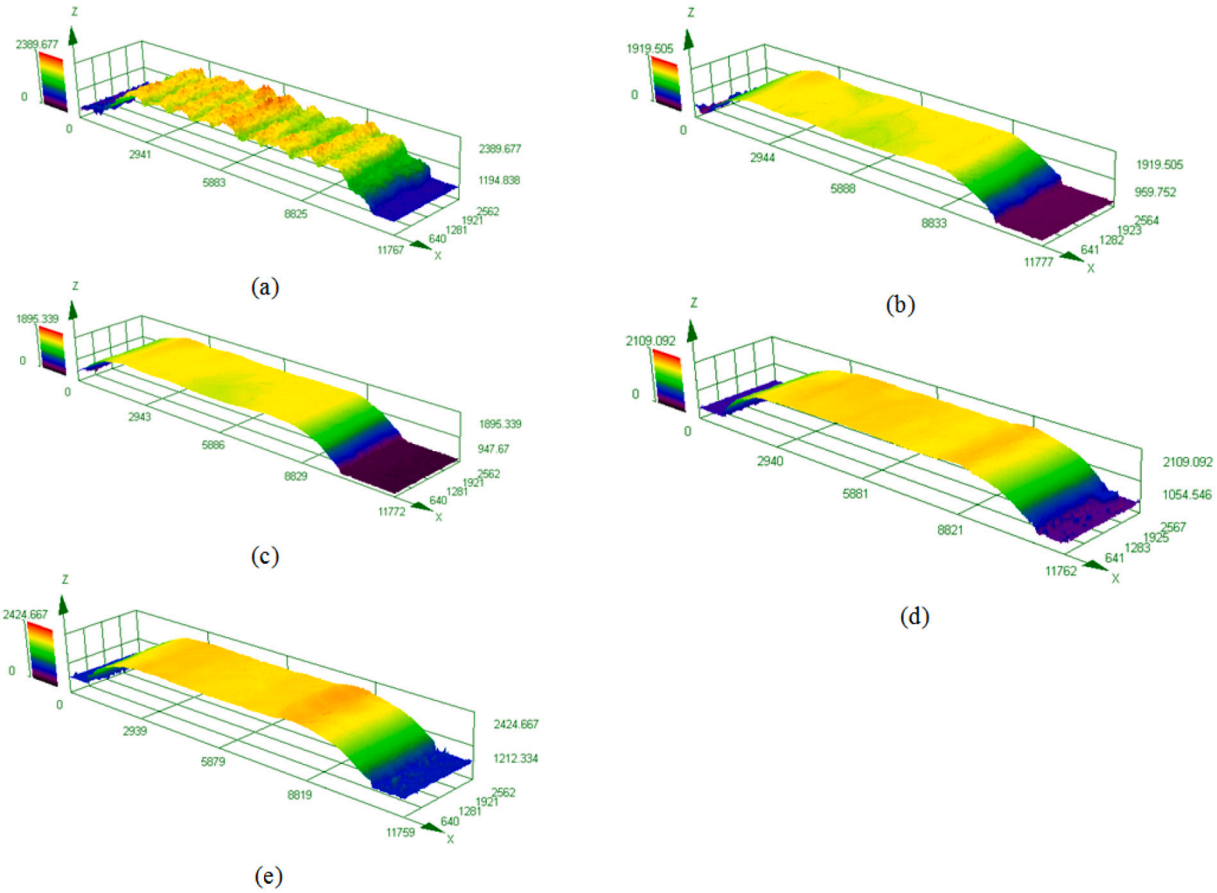

Fig. 3. Three-dimensional optical profile of the cladding layer of (a) sample No.1, (b) sample No.2, (c) sample No.3, (d) sample No.4 and (e) sample No.5.

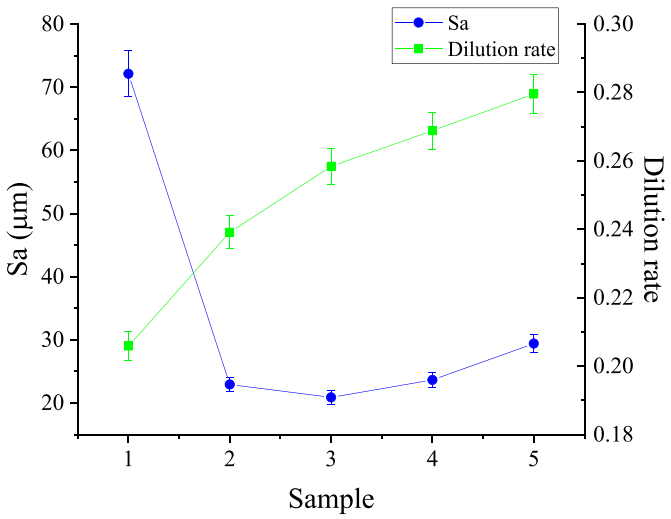

Fig. 4. Surface roughness and dilution rate of cladding layer with different samples.

lower than that without laser re-melting. However, the surface roughness of cladding layer does not decrease with the increase of laser power, but takes on a tendency of decreasing first and then increasing. The most probable cause of this phenomenon is that laser re-melting can indeed re-melt the incompletely melted parts in the cladding layer and the incompletely melted particulate alloy powders on the surface, leading to the lower surface roughness. However, with the increase of laser power, the heat energy input into the cladding zone increases, which leads to the increase of temperature gradient. Therefore, the residual stress increases [23]. Moreover, the residual stress in the coating area is mainly compressive residual stress, which increases significantly along the transverse, longitudinal and normal directions with the increase of the laser power [24]. Therefore, as the residual compressive stress increases, the warpage and the surface roughness of the cladding layer increase.

3.2. Dilution rate of different samples

Dilution rate is a key factor to measure the properties of the cladding layer:

$$\lambda = \frac{D}{(H + D)} \tag{1}$$

where H is the clad height, and D is the melting pool depth.

As shown in Fig. 4, the dilution rate of cladding layer after different laser power re-melting is higher than that without laser re-melting, and the dilution rate increases if re-melting laser power increases. This phenomenon is caused by the increase of re-melting laser power, and the fusion between cladding layer and substrate is more sufficient, resulting in an increase of dilution rate. Therefore, laser re-melting is not suitable for heat sensitive materials.

3.3. Cross section morphology of different samples

Fig. 5 shows the cross section morphology of different samples. As shown in Fig. 5(a), there are cracks and defects in the cross section of the cladding layer without laser re-melting, and there are many "grooves" between each cladding track. This phenomenon is due to the fact that the laser cladding is a process of rapid melting and solidification. High residual stress often exists in the cladding layer, leading to the formation of the cracks and pores. Moreover, the overlapping zone is at the edge of the laser beam with lower energy density, and less energy is obtained from the laser, resulting in less melted powder than other zones. Therefore, there exists grooves in the overlapping zone of sample No.1. As seen from Fig. 5(b) and (c), when the re-melting laser power is changed from 550 W to 750 W, no cracks and defects are observed in the cross section of cladding layer. However, when the re-melting laser power is 850 W, the cracks exist again in the cross section. This phenomenon is due to the increase of temperature gradient with the increase of re-melting laser power, which leads to the increase of residual stress. As a result, cracks appeared in the cladding layer of Sample No.5. Moreover, it is indicated that laser re-melting can eliminate defects in the cladding layer. However, excessive re-melting laser power causes defects to form again in the cladding layer.

3.4. Microstructure of different samples

Fig. 6 shows a part of the cross section morphology of different samples. As shown in Fig. 6(a), (e) and (i), a large number of equiaxed

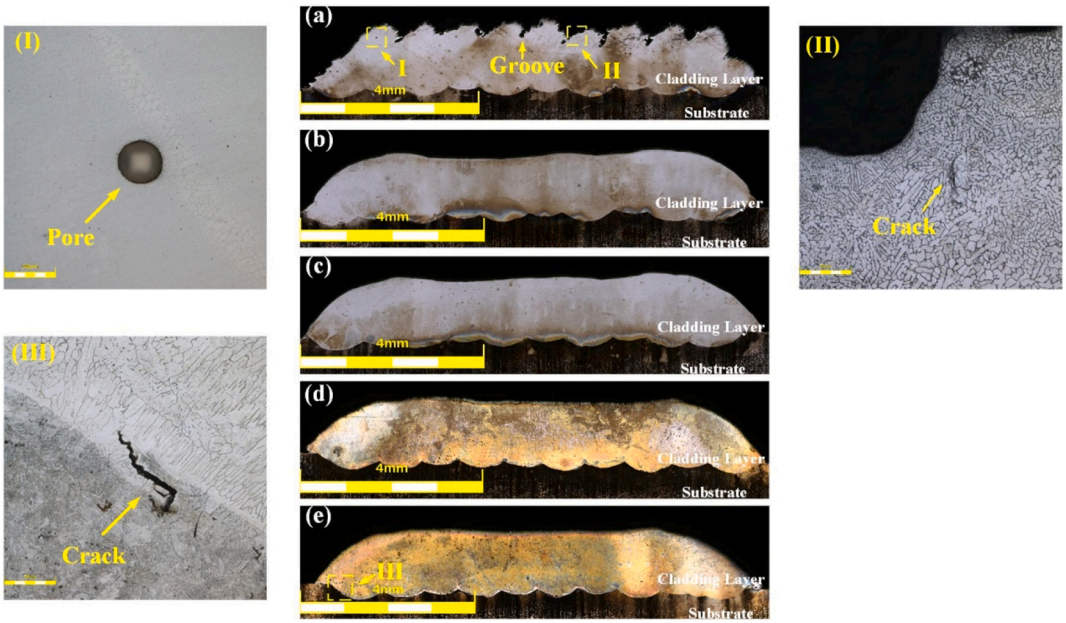

Fig. 5. Cross section morphology of (a) sample No.1, (b) sample No.2, (c) sample No.3, (d) sample No.4 and (e) sample No.5.

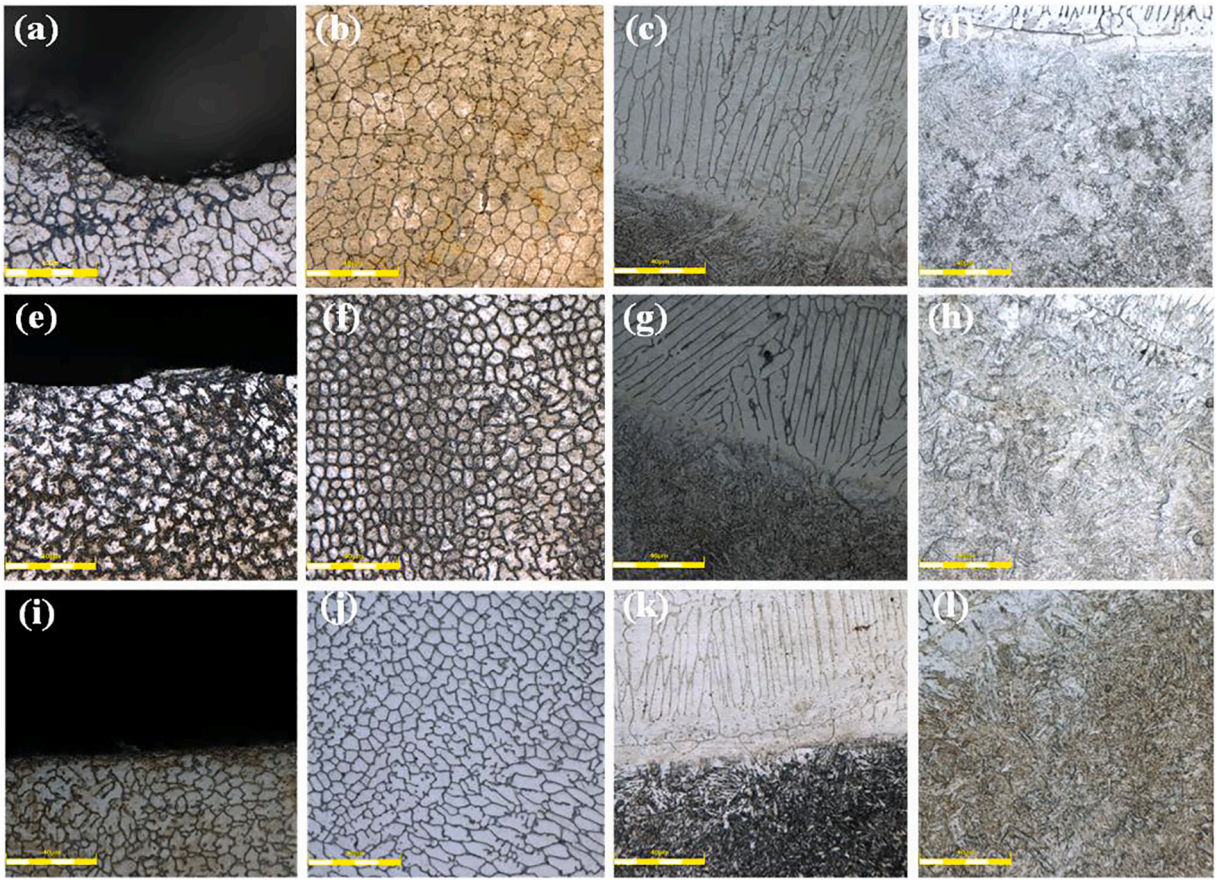

Fig. 6. Microstructure of (a) top of sample No.1, (b) middle of sample No.1, (c) Bottom of sample No.1, (d) heat affected zone of sample No.1 (e) top of sample No.3, (f) middle of sample No.3, (g) Bottom of sample No.3, (h) heat affected zone of sample No.3 (i) top of sample No.5, (j) middle of sample No.5, (k) Bottom of sample No.5, (l) heat affected zone of sample No.5.

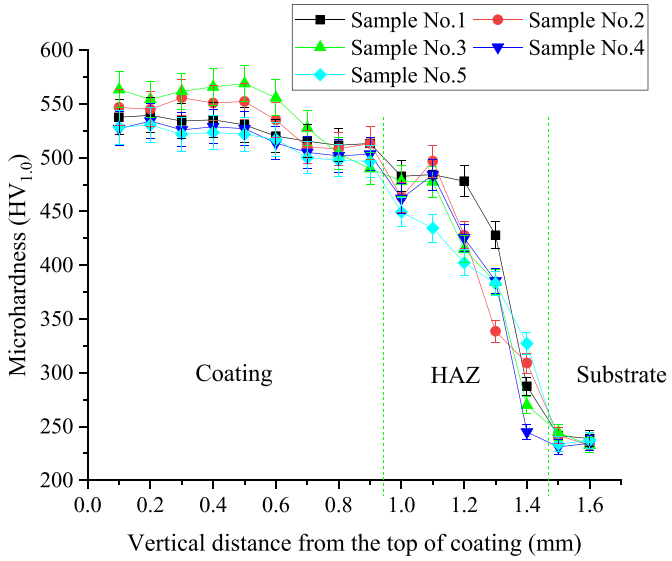

Fig. 7. Microhardness distribution along the cross section depth of coating.

crystals are formed in the top of the cladding layer. Shielding gas and powder feeding gas have little effect on heat dissipation, resulting in the growth speed of crystal nucleus in all directions is basically same. Therefore, the phenomenon mentioned earlier occurs. Fig. 6(b), (f) and (j) show the middle of the cross section morphology of different samples, and a large number of uniform equiaxed crystals are formed in the middle of the cladding layer. Since the distance between the middle of the cladding layer and the substrate is relatively long, and the temperature gradient is relatively small. The growth speed of crystal nucleus in all directions is basically same. Therefore, a large number of uniform equiaxed crystals are formed in the middle of cladding layer. As shown in Fig. 6(c), (g) and (k), a large number of columnar crystals are formed in the bottom of cladding layer. The cause of this phenomenon is that the distance between the bottom of cladding layer and substrate is close, and the temperature gradient is large, leading to a large number of columnar crystals. As shown in Fig. 6(d), (h) and (l), during the laser cladding and laser re-melting process, the substrate near the bottom of melting pool is heated to the recrystallization temperature. When the substrate is cooled to room temperature, the martensite transformation occurs to form lath martensite. In summary, with the increase of re-melting laser power, the grain size in each zone of cladding layer changed, but the grain type did not change. It is indicated that re-melting laser power has little effect on the distribution pattern of the crystals in the cladding layer.

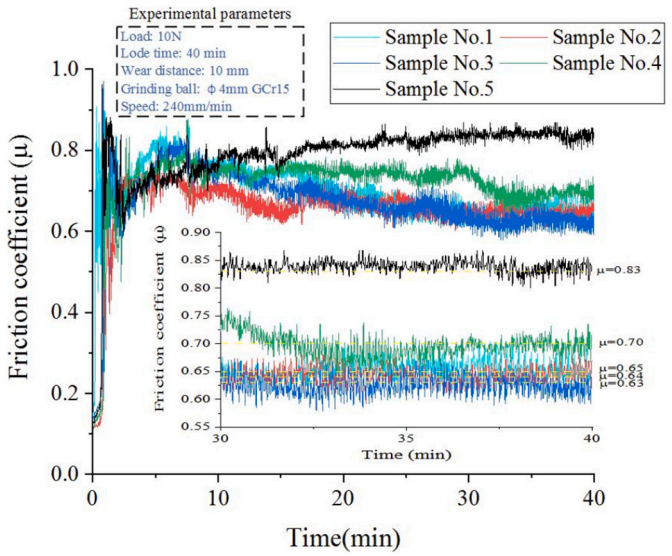

Fig. 8. Friction coefficient curves of different samples.

3.5. Mechanical properties of different samples

Fig. 7 shows the microhardness distribution along the cross section depth of different samples. As shown in Fig. 7, the average microhardness of the coating with different samples are followed in the given order: sample No.3(543$HV_{1.0}$) > sample No.2(535$HV_{1.0}$) > sample No.1 (526$HV_{1.0}$) > sample No.4(518$HV_{1.0}$) > sample No.5(515$HV_{1.0}$), and the average microhardness of sample No.3 coating is 2.3 times that of substrate. According to the results of dilution rate and microstructure of different coatings, when the re-melting laser power is increased from 550 W to 650 W, the dilution rate shows a downward trend and the defects in the coating disappear. Moreover, the size of crystal grains inside coating becomes smaller. Therefore, due to the effect of fine-grain strengthening, the microhardness of coating with sample No.1, 2 and 3 is increased. When the re-melting laser power is increased from 750 W to 850 W, the dilution rate shows an upward trend and defects in the coating appear. At the same time, the size of crystal grains inside coating becomes larger. It may be due to heat accumulation under laser re-melting. When the re-melting laser power is relatively high, the accumulated heat makes the temperature difference of coating smaller and leads to the decrease of cooling rate, resulting in a coarse crystal phase. Therefore, the microhardness of the coating with sample No.4 and 5 shows a downward trend. In addition, Fig. 7 shows that the average microhardness of heat affected zone (HAZ) is significantly higher than that of substrate, which may be due to the effect of fine-grain strengthening and solid solution strengthening.

Wear resistance is one of the most important macroscopic features of cladding layer. Therefore, the wear resistance of each sample was evaluated by the friction coefficient, wear morphology and wear rate. In order to objectively reflect the wear resistance of each sample, each sample was tested under the same experimental conditions. Fig. 8 shows the friction coefficient curves of different samples. It is noticed that the friction coefficients of different samples fluctuate greatly at the beginning, but the friction coefficients of different samples tend to be stable after a period of wear. In this paper, the friction coefficient of each sample is selected from 30 min to 40 min to calculate the average friction coefficient. As shown in Figs. 8 and 9, the average friction coefficients and wear rate of different samples are both followed in the given order: sample No.3 < sample No.2 < sample No.1 < sample No.4 < sample No.5. When the re-melting laser power is 650 W, the wear rate and the average friction coefficient of the cladding layer are minimum value, which shows that the wear resistance of sample No.3 is the most

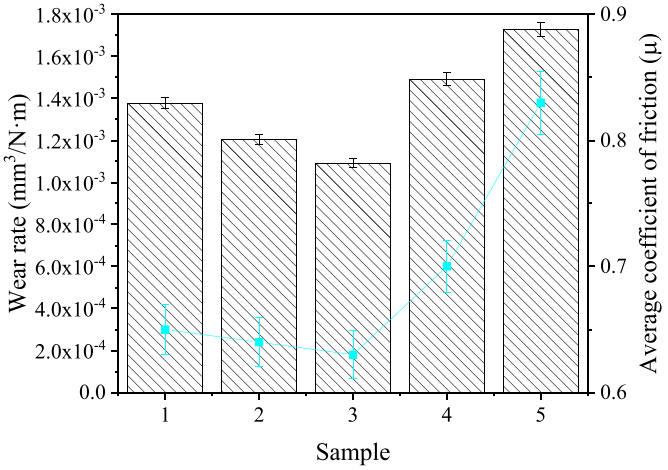

Fig. 9. The wear rate and average friction coefficient of different samples.

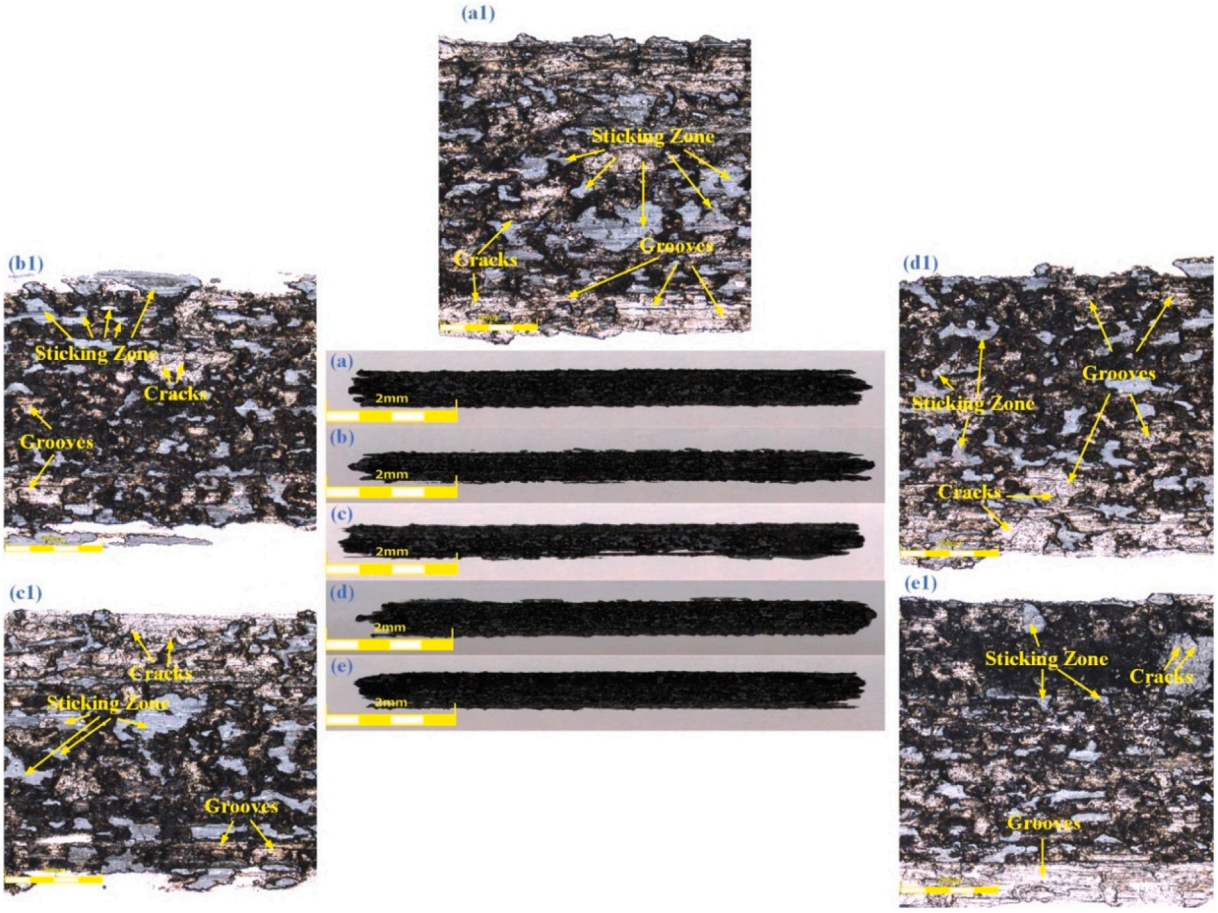

Fig. 10. Wear morphology of (a) sample No.1, (b) sample No.2, (c) sample No.3, (d) sample No.4 and (e) sample No.5.

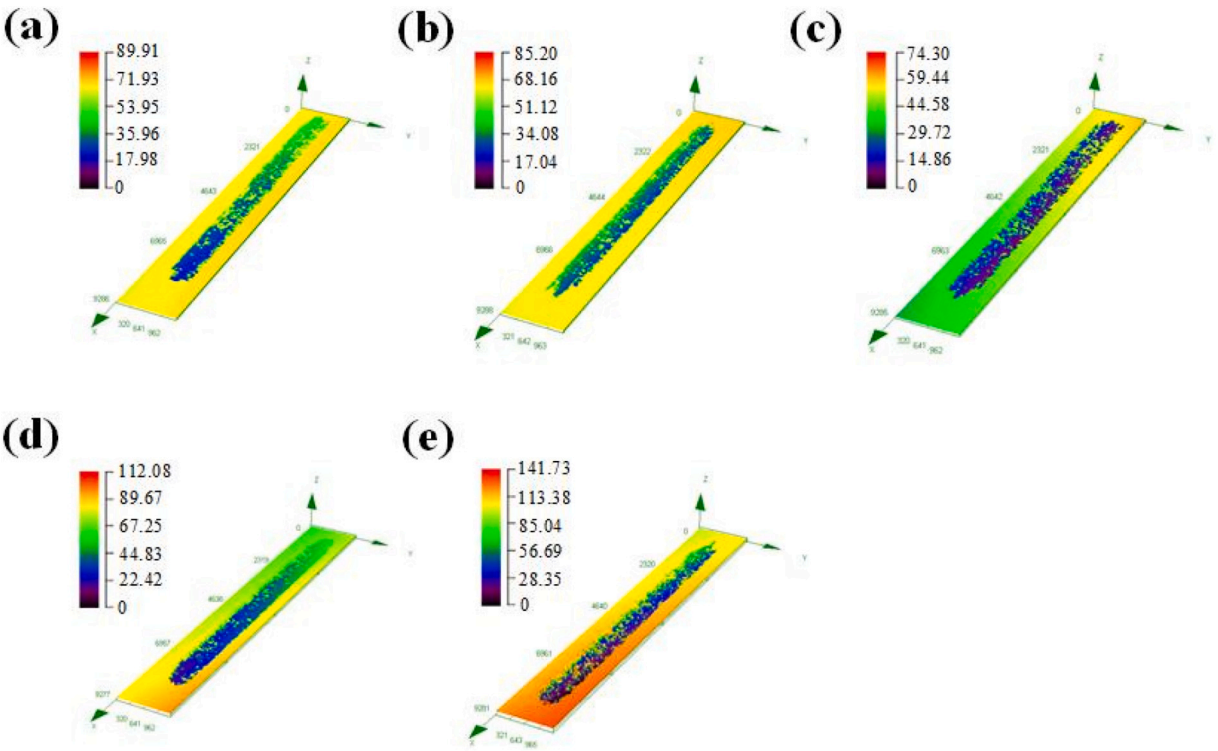

Fig. 11. Three-dimensional wear morphology of (a) sample No.1, (b) sample No.2, (c) sample No.3, (d) sample No.4 and (e) sample No.5.

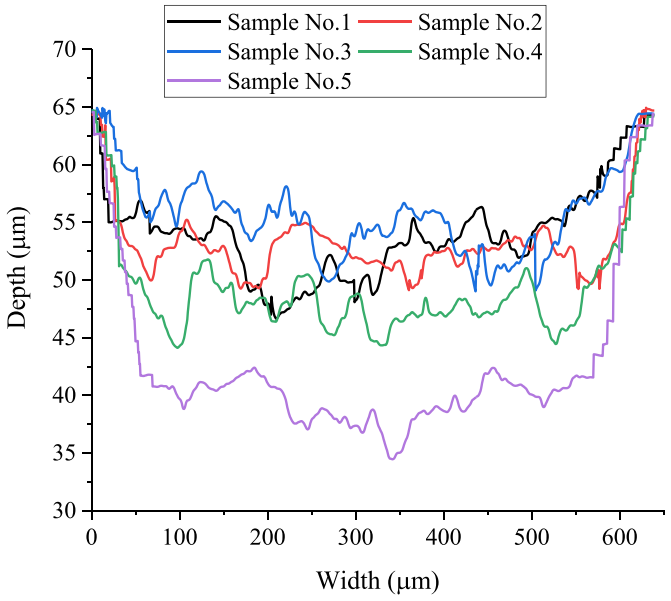

Fig. 12. Wear cross section profiles of different samples.

excellent. This result is due to the fact that the cladding layer of sample No.3 has the highest microhardness and no defects in the cladding layer. In addition, the average friction coefficient of sample No.3 is 0.76 times than that of sample No.5, and the wear rate of sample No.3 is 0.63 times than that of sample No.5, which indicates that the re-melting laser power has a great effect on the wear resistance of the cladding layer.

Figs. 10 and 11 show the wear morphology of each sample. As shown in Figs. 10 and 11, there are many grooves, smooth wear surfaces, spalled pits and cracks on the wear morphology, which indicates that the wear form of each sample is the combination of abrasive wear, adhesive wear and fatigue wear. In addition, as shown in Figs. 10 and 12, the wear depth and width decrease first and then increase, wherein the wear depth and width of sample No.3 is the smallest and sample No.5 is the largest. When the load is remaining constant, the crushed surface area decreases if microhardness increases. Therefore, when the microhardness tends to increase, the wear depth and width tend to decrease.

4. Conclusions

In summary, re-melting under different laser power conditions was carried out on YCF102 cladding layer, and the morphology and mechanical properties were studied. *Re*-melting laser power has little effect on the distribution of the crystals in the cladding layer, but it causes grain refinement. In addition, laser re-melting can not only improve the surface morphology of cladding layer, but also reduce the number of defects and improve the mechanical properties. However, excessive re-melting laser power leads to the increase of dilution rate and the formation of defects, which result in the degradation of the performance. When the re-melting laser power is 650 W, the microhardness of cladding layer is 2.3 times than that of the substrate, and the average friction coefficient and wear rate are 0.76 times and 0.63 times than that of YCF102 cladding layer after re-melting at the laser power of 850 W respectively.

CRediT authorship contribution statement

Wenchao Xi: Conceptualization, Investigation, Writing – original draft, Writing – review & editing. **Boxue Song:** Validation, Writing – review & editing. **Zixuan Wang:** Validation, Writing – review & editing. **Tianbiao Yu:** Resources, Supervision, Project administration, Funding acquisition. **Jun Wang:** Resources, Supervision. **Yuanxing Dai:** Validation.

Declaration of competing interest

The authors declare that they have no known competing financial interests or personal relationships that could have appeared to influence the work reported in this paper.

Acknowledgments

This work was supported by 2016 Green Manufacturing System Integration Project of Ministry of Industry and Information Technology of China [grant number 201675514]; Liaoning Provincial Key Laboratory of Large Equipment Intelligent Design and Manufacturing Technology [grant number 18006001].

References

[1] F. Weng, C. Chen, H. Yu, Research status of laser cladding on titanium and its alloys: a review, Mater. Des. 58 (2014) 412–425, https://doi.org/10.1016/j.matdes.2014.01.077.
[2] K.A. Chiang, Y.C. Chen, Microstructural characterization and microscopy analysis of laser cladding Stellite12 and tungsten carbide, J. Mater. Process. Technol. 182 (2007) 297–302, https://doi.org/10.1016/j.jmatprotec.2006.08.007.
[3] J. Liu, H. Yu, C. Chen, F. Weng, J. Dai, Research and development status of laser cladding on magnesium alloys: a review, Opt. Lasers Eng. 93 (2017) 195–210, https://doi.org/10.1016/j.optlaseng.2017.02.007.
[4] P. Zhang, Z. Liu, Effect of sequential turning and burnishing on the surface integrity of Cr-Ni-based stainless steel formed by laser cladding process, Surf. Coat. Technol. 276 (2015) 327–335, https://doi.org/10.1016/j.surfcoat.2015.07.026.
[5] L. Ding, S. Hu, X. Quan, J. Shen, Effect of Mo and nano-Nd2O3 on the microstructure and wear resistance of laser cladding Ni-based alloy coatings, Appl. Phys. A Mater. Sci. Process. 122 (2016), https://doi.org/10.1007/s00339-016-9905-1.
[6] S. Kumar, A. Mandal, A.K. Das, A.R. Dixit, Parametric study and characterization of AlN-Ni-Ti6Al4V composite cladding on titanium alloy, Surf. Coat. Technol. 349 (2018) 37–49, https://doi.org/10.1016/j.surfcoat.2018.05.053.
[7] A. Emamian, S.F. Corbin, A. Khajepour, Effect of laser cladding process parameters on clad quality and in-situ formed microstructure of Fe-TiC composite coatings, Surf. Coat. Technol. 205 (2010) 2007–2015, https://doi.org/10.1016/j.surfcoat.2010.08.087.
[8] B.A. Khamidullin, I.V. Tsivilskiy, A.I. Gorunov, A.K. Gilmutdinov, Modeling of the effect of powder parameters on laser cladding using coaxial nozzle, Surf. Coat. Technol. 364 (2019) 430–443, https://doi.org/10.1016/j.surfcoat.2018.12.002.
[9] M. Erfanmanesh, R. Shoja-Razavi, H. Abdollah-Pour, H. Mohammadian-Semnani, Influence of using electroless Ni-P coated WC-Co powder on laser cladding of stainless steel, Surf. Coat. Technol. 348 (2018) 41–54, https://doi.org/10.1016/j.surfcoat.2018.05.016.
[10] J.C. Heigel, M.F. Gouge, P. Michaleris, T.A. Palmer, Selection of powder or wire feedstock material for the laser cladding of Inconel® 625, J. Mater. Process. Technol. 231 (2016) 357–365, https://doi.org/10.1016/j.jmatprotec.2016.01.004.
[11] X.G. Hu, Q. Zhu, H.X. Lu, F. Zhang, D.Q. Li, S.P. Midson, Microstructural evolution and thixoformability of semi-solid aluminum 319s alloy during re-melting, J. Alloys Compd. 649 (2015) 204–210, https://doi.org/10.1016/j.jallcom.2015.07.121.
[12] W. Yu, S.L. Sing, C.K. Chua, X. Tian, Influence of re-melting on surface roughness and porosity of AlSi10Mg parts fabricated by selective laser melting, J. Alloys Compd. 792 (2019) 574–581, https://doi.org/10.1016/j.jallcom.2019.04.017.
[13] Y. Li, S. Dong, S. Yan, X. Liu, E. Li, P. He, B. Xu, Elimination of voids by laser remelting during laser cladding Ni based alloy on gray cast iron, Opt. Laser Technol. 112 (2019) 30–38, https://doi.org/10.1016/j.optlastec.2018.10.055.
[14] W. Gao, S. Zhao, Y. Wang, F. Liu, C. Zhou, X. Lin, Effect of re-melting on the cladding coating of Fe-based composite powder, Mater. Des. 64 (2014) 490–496, https://doi.org/10.1016/j.matdes.2014.08.004.
[15] G. Sun, Y. Zhang, C. Liu, Effects of laser surface re-melting on the microstructure and hardness of laser deposited Co-285+WC coatings, Lasers Eng. 20 (2010) 9–20.
[16] W. Gao, S. Zhao, Y. Wang, Z. Zhang, C. Zhou, X. Lin, Refinement of Fe-based alloy doped Ti cladding layer, Surf. Coat. Technol. 270 (2015) 16–23, https://doi.org/10.1016/j.surfcoat.2015.03.024.
[17] Z. Cai, X. Cui, Z. Liu, Y. Li, M. Dong, G. Jin, Microstructure and wear resistance of laser cladded Ni-Cr-Co-Ti-V high-entropy alloy coating after laser remelting processing, Opt. Laser Technol. 99 (2018) 276–281, https://doi.org/10.1016/j.optlastec.2017.09.012.
[18] Y. Yao, X. Li, Y.Y. Wang, W. Zhao, G. Li, R.P. Liu, Microstructural evolution and mechanical properties of Ti-Zr beta titanium alloy after laser surface remelting, J. Alloys Compd. 583 (2014) 43–47, https://doi.org/10.1016/j.jallcom.2013.08.160.
[19] V.K. Balla, J. Soderlind, S. Bose, A. Bandyopadhyay, Microstructure, mechanical and wear properties of laser surface melted Ti6Al4V alloy, J. Mech. Behav. Biomed. Mater. 32 (2014) 335–344, https://doi.org/10.1016/j.jmbbm.2013.12.001.

[20] B. Vamsi Krishna, A. Bandyopadhyay, Surface modification of AISI 410 stainless steel using laser engineered net shaping (LENSTM), Mater. Des. 30 (2009) 1490–1496, https://doi.org/10.1016/j.matdes.2008.08.003.
[21] S. Zhou, Y. Xu, B. Liao, Y. Sun, X. Dai, J. Yang, Z. Li, Effect of laser remelting on microstructure and properties of WC reinforced Fe-based amorphous composite coatings by laser cladding, Opt. Laser Technol. 103 (2018) 8–16, https://doi.org/10.1016/j.optlastec.2018.01.024.
[22] B. Xin, X. Zhou, G. Cheng, J. Yao, Y. Gong, Microstructure and mechanical properties of thin-wall structure by hybrid laser metal deposition and laser remelting process, Opt. Laser Technol. 127 (2020), https://doi.org/10.1016/j.optlastec.2020.106087.
[23] M. Song, L. Wu, J. Liu, Y. Hu, Effects of laser cladding on crack resistance improvement for aluminum alloy used in aircraft skin, Opt. Laser Technol. 133 (2021), https://doi.org/10.1016/j.optlastec.2020.106531.
[24] T. Roy, A. Paradowska, R. Abrahams, M. Law, P. Mutton, M. Soodi, W. Yan, Residual stress in laser cladded heavy-haul rails investigated by neutron diffraction, J. Mater. Process. Technol. 278 (2020), https://doi.org/10.1016/j.jmatprotec.2019.116511.